

Technical Notes

TECHNICAL NOTES are short manuscripts describing new developments or important results of a preliminary nature. These Notes cannot exceed 6 manuscript pages and 3 figures; a page of text may be substituted for a figure and vice versa. After informal review by the editors, they may be published within a few months of the date of receipt. Style requirements are the same as for regular contributions (see inside back cover).

Conjugate Forced Convection Heat Transfer in Tubes with Obstruction

M. Ruhul Amin*

Montana State University, Bozeman, Montana 59717

Introduction

IN the design of heat transfer equipment, the knowledge of the amount of heat transfer and temperature distribution is very important to prevent thermally induced failure. Since the first publication of the so-called Graetz problem, there have been many studies on laminar flow in circular tubes.¹ Laminar flow occurs in a tube because of small dimensions, low flow rates, or highly viscous fluids. Compact heat exchangers represent the industrial situation where laminar flow is encountered. Although important, but most often ignored, is the effect of conjugation, that is, coupling of conduction and convection. Wall conduction becomes an important factor when the thickness of the pipe cannot be neglected in comparison to pipe radius. As described by Perelman,² heat transfer problems involving multimaterial solid domains, localized heat generation, and complex fluid flow behavior including separation and reattachment, can involve conjugation.

In a heat exchanger tube, conduction is present not only through the tube wall, but also through the deposits accumulated on the wall surface because of fouling. Fouling reduces the heat transfer rate as a result of an increase in fluid friction and thermal resistance and, thus, increases both the initial and operating costs of heat exchangers. The deposits also restrict the flow passage of the tube. This restriction is often more in some places than in other places. This study is concerned with the conjugate heat transfer in a circular tube with an obstruction. The tube geometry is shown in Fig. 1. In addition to the wall conduction, the flow is restricted by an obstruction on the tube wall. A uniform wall temperature is assigned as the boundary condition because this type of condition is more prevalent in process industry applications. The fluid enters the tube with a uniform inlet temperature and a parabolic velocity profile is assigned as the inlet boundary condition.

Numerical Approach

A finite element method based on Galerkin technique³ was used for the current analysis. Two-dimensional continuity, Navier–Stokes, and energy equations were solved simultaneously. The flow was assumed to be laminar, axisymmetrical with negligible buoyancy force and viscous dissipation. All of the physical properties were assumed to be constant. Because of the conjugate heat transfer at the solid–fluid interface, the continuity of the temperature and heat flux was satisfied at the interface. The outside radius of the tube is r_o and the tube

length is equal to $13.33r_o$. The minimum flow passage caused by obstruction is located at a distance equal to $3.33r_o$. At the entrance and exit of the tube, the inside radius is equal to $0.833r_o$. At the location of the minimum flow passage, the inside radius is equal to $0.417r_o$.

Results are expressed in terms of dimensionless local heat flux along the solid–fluid interface, $\Phi_x = 2q''_x r_o / k_f (T_o - T_{in})$, Reynolds number, $Re = 2Vr_o \rho / \mu$, thermal conductivity ratio, $k_r = k_s / k_f$. Where q''_x , k_f , k_s , T_o , T_{in} , V , ρ , and μ are local heat flux along the interface, thermal conductivity of the fluid, thermal conductivity of the solid, outside wall temperature, fluid inlet temperature, average fluid velocity at the inlet, fluid density and fluid viscosity, respectively. The average dimensionless heat flux Φ was determined by integrating Φ_x along the solid–fluid interface. The computer code was tested for its accuracy by comparing the results with other benchmark solutions. A grid independency test was also conducted. Details of the code validation tests are documented in Amin.⁴

Results and Discussion

In this research, the ranges of Reynolds number Re and solid–fluid thermal conductivity ratio k_r considered were $1 \times 10^2 - 6 \times 10^2$ and $0.03 - 10.0$ respectively. A fluid Prandtl number Pr of 7.56 was used. Figure 2 shows the streamlines for cases with $k_r = 0.3$ and $Re = 1 \times 10^2$, 3×10^2 , and 6×10^2 . At low Re values, recirculation past the obstruction is either too weak to plot, or has not started. However, with the increase of Re , the recirculation starts and extends all the way up to and beyond the tube exit for higher values of Re . From the radial velocity profile (not shown here), it is seen that backflow (negative velocity) occurs in the tube because of recirculation. From the radial velocity profile it is also seen that because of the presence of the obstruction, the parabolic nature of the inlet fluid turns to elliptic (past the obstruction). For low Re flow, the flow again becomes fully developed and parabolic at the exit of the tube. However, for high Re cases, the flow remains elliptic. A similar trend is observed for all the cases with different values of k_r .

Figure 3 shows the nondimensional average heat flux Φ for different cases run for the purpose of this study. As a result of recirculation at higher values of Re , the average heat flux increases initially, and then decreases with Re increase. This trend is observed for all values of k_r . However, with higher values of k_r (>1), the decrease in Φ at higher Re values occurs later than the cases with lower values of k_r (<1). This is because the retardation of heat transfer rate caused by recirculation flow is smaller than the enhancement of heat transfer rate caused by the increased value of the tube wall thermal conductivity k_s . From Fig. 3 it can also be seen that for $k_r = 0.03$, the average heat flux is almost independent of Re . This is because at this value of k_r , the entire fluid region is isothermal. Temperature gradients exist inside the solid region only. In this case, the heat transfer resistance due to convection (in the fluid region) is much lower compared to the corresponding resistance due to conduction (in the solid region). Therefore, the average heat transfer rate has very little or no effect on the flow condition inside the tube. At higher values of k_r , the reverse, that is, greater dependency of heat transfer rate with change of Reynolds number, is true, and its effects can be seen in Fig. 3.

Received Oct. 25, 1996; received Sept. 16, 1997; accepted for publication Sept. 17, 1997. Copyright © 1997 by the American Institute of Aeronautics and Astronautics, Inc. All rights reserved.

*Associate Professor, Department of Mechanical and Industrial Engineering.

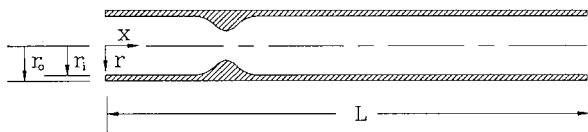


Fig. 1 Investigated geometry.

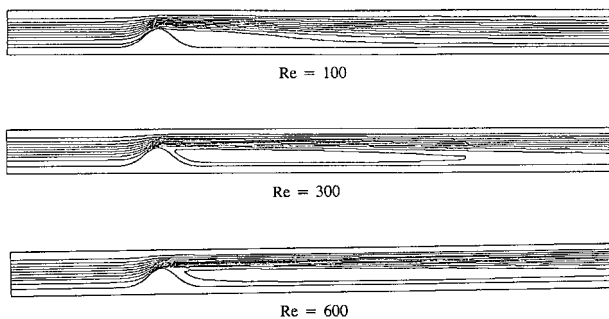
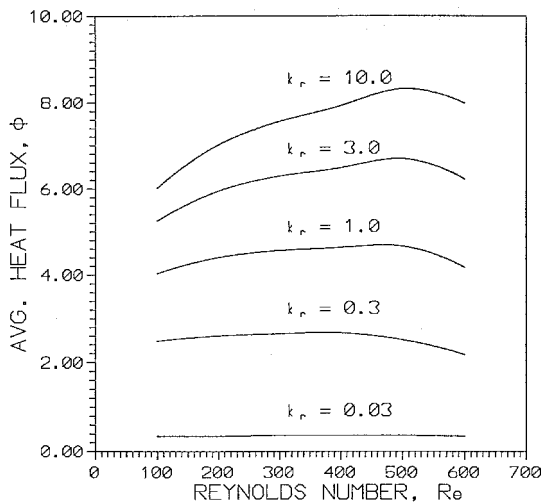
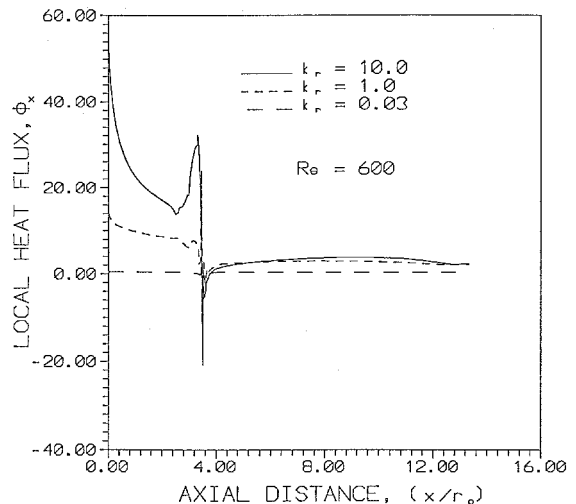
Fig. 2 Streamlines for cases with $k_r = 0.3$.Fig. 3 Average heat flux distribution for different values of k_r .

Figure 4 shows the local nondimensional heat flux Φ_x along the inner wall of the tube with $Re = 6 \times 10^2$ and for different values of k_r . It can be seen that Φ_x decreases as the fluid travels in the axial direction. At later locations, as the fluid velocity increases because of decreased flow area, the local heat transfer rate starts to increase. It reaches its maximum value at the tip of the obstruction (location of maximum fluid velocity). Past the obstruction tip, a sharp drop in the heat transfer occurs. This is because of the reduced flow and the creation of a recirculation zone. Further downstream, Φ_x slowly arrives at a stable value. A similar trend is observed for other Re values. For $k_r < 1$, almost constant heat transfer occurs throughout the entire length of the tube, except near the tip of the obstruction. As can be seen in Fig. 4, the local heat transfer rate fluctuates near the obstruction tip because of increased and decreased fluid velocity.

It can also be seen from Fig. 4 that past the obstruction tip, the value of Φ_x becomes negative in some places. This is because in the recirculating zone, right after the obstruction tip, the shear layer prohibits convective exchange between the heated recirculating fluid and the relatively cooler tube fluid. On the other hand, the recirculation fluid is being continuously heated by the tube wall downstream. As a result, just after the obstruction tip, the recirculating fluid becomes hotter than the adjacent inner wall of the tube. This leads to heat transfer into, rather than out of the tube wall. However, further downstream, the shear layer is disrupted, some of the heated fluid is replaced

Fig. 4 Local heat flux distribution for different values of k_r .

by the cooler tube fluid, and convective exchange takes place. As such, Φ_x plunges back to positive values. It is interesting to note that a similar trend is reported by Nigen and Amon⁵ for conjugate heat transfer with recirculation flow in grooved channels.

Conclusions

From the numerical investigation of the present study, it is observed that because of the presence of an obstruction, the parabolic nature of the inlet fluid turns to elliptic. For low Reynolds number flow, the flow again becomes fully developed and parabolic at the exit of the tube. However, for high Re flow, the flow remains elliptic. At higher Re values, recirculation flow occurs past the obstruction. This recirculation causes a reversal of the direction of heat flow at certain locations along the tube wall. From the isotherm plots it is observed that for low values of the thermal conductivity ratio, the entire fluid region in the tube remains isothermal and the total heat transfer is less dependent on Re . For the cases with high values of thermal conductivity ratio, almost the entire solid wall remains isothermal and the temperature gradients are in the fluid region. The total heat transfer rate from the tube increases up to a certain value of the Re increase. Past this value, the heat transfer decreases with the Re increase. Near the obstruction, the local heat flux values fluctuate as a result of recirculation flow. The local temperature of the obstructed wall also changes with a big jump near the obstruction. Because of recirculation, backflow (negative velocity) occurs in the tube. This is more prominent at higher Re values.

Acknowledgment

Computer simulations of this study were conducted on the Cray C90 supercomputer at the Pittsburgh Supercomputing Center under Grant CTS920010P.

References

- ¹Shah, R. K., and London, A. L., *Laminar Flow Forced Convection in Ducts*, Supplement 1 to *Advances in Heat Transfer*, Academic, New York, 1978.
- ²Perelman, T. L., "On Conjugate Problems of Heat Transfer," *International Journal of Heat and Mass Transfer*, Vol. 3, No. 4, 1961, pp. 293–303.
- ³Gartling, D. K., *NACHOS II—A Finite Element Computer Program for Incompressible Flow Problems, Part I—Theoretical Background*, Sandia Labs., SAND86-1816, UC-32, Albuquerque, NM, 1987.
- ⁴Amin, M. R., "Conjugate Forced Convection Heat Transfer in Tubes with Obstructions," *Proceedings of the ASME/JSME Thermal Engineering Joint Conference*, Vol. 1, American Society of Mechanical Engineers, New York, 1995, pp. 261–268.

Nigen, J. S., and Amon, C. H., "Effect of Material Composition and Localized Heat Generation on Conjugate Heat Transport in Grooved Channels," American Society of Mechanical Engineers, Paper 93-WA/HT-15, Nov. 1993.

Effect of Rib Profiles on Turbulent Channel Flow Heat Transfer

Pankaj R. Chandra* and Michael L. Fontenot*

McNeese State University,
Lake Charles, Louisiana 70609

and

Je-Chin Han*

Texas A&M University, College Station, Texas 77843

Introduction

REPEATED ribs have been used as the promoters of turbulence to enhance the heat transfer to the flow of coolants in channels. Several publications have addressed the comprehensive review of turbine blade cooling and the analysis of heat transfer and friction characteristics of flow in channels with two opposite rib-roughened walls. The effects of flow Reynolds number and rib geometry (rib height e , rib spacing P , rib angle of attack α , and rib orientation) on heat transfer and pressure drop in the fully developed region of square, rectangular, and triangular channels have been investigated.¹⁻⁴ Semiempirical correlations over a wide range of rib geometry for the friction and heat transfer design calculations are derived from the law-of-the-wall similarity for flow over rough surfaces. A detailed analysis of the application of the similarity laws in the case of rectangular channels is presented by Han.^{1,2} Also, studies of the effect of a number of channel-ribbed walls on heat and friction characteristics have been reported.^{5,6}

Experiments with some nonrectangular rib shapes have been reported.^{7,8} The previously mentioned studies were limited in the number of rib shapes and were for different conditions (rib height to channel hydraulic diameter ratio e/D_h , and Reynolds number Re). This study focuses on the effect of different rib profiles on turbulent channel flow heat transfer and friction characteristics.

Experimental Setup and Procedure

The test channel is a 5.08×5.08 cm square cross section (Fig. 1a) and is 101.6 cm long. The test channel is made of 10 10.16-cm-long sections of 0.64-cm-thick copper plates, separated by 0.08-cm-thick balsa wood to reduce both the streamwise and circumferential heat conduction effects. Copper ribs with a height of 0.64 cm ($e/D_h = 0.125$), and equally spaced at 6.4 cm ($P/e = 10$), are glued with silicone adhesive onto the two opposite walls of the channel (Fig. 1b). Rib profiles are shown in Fig. 1c. The walls are heated individually with electric strip heaters, which are embedded and flatly placed between the copper and wood plates to ensure good contact. Heaters are independently controlled by a transformer and provide a constant heat flux to the walls. Each section of the walls has a thermocouple in the center. The test section is enclosed by 3.81-cm-thick styrofoam insulation.

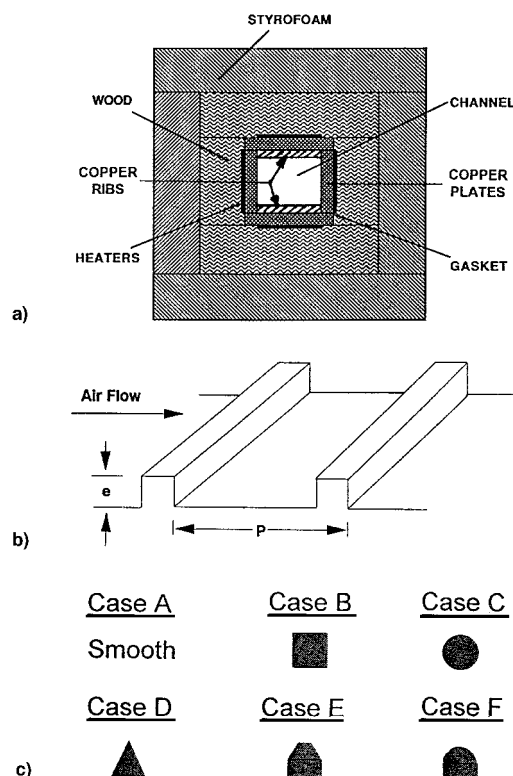


Fig. 1 a) Cross section of test channel, b) ribbed wall geometry, and c) cases with varying rib profiles.

Temperatures of the air entering and leaving the test channel are the average values of the readings recorded by a traversing probe. When thermal steady state is reached and the temperature of the four sections at any cross section of the channel is about the same, temperature and pressure data are recorded. Details are available in Refs. 5 and 6. The same procedure is repeated for the range of Reynolds numbers and for all rib configurations.

Data Reduction

Reference 6 may be referred to for the equations to calculate friction factor f , and the local heat transfer coefficient based on the area of a smooth channel h . The friction factor and Nusselt number are normalized by the respective values of the friction factor f_0 , and Nusselt number Nu_0 , for fully developed smooth pipe turbulent flow.

The maximum uncertainties in the heat transfer coefficient and friction factor are estimated to be ± 7 and $\pm 8\%$, respectively, using the uncertainty estimation method of Kline and McClintock.⁹ The maximum heat loss to the atmosphere is about 6% of the total heat supplied to the channel walls.

For turbulent flow in square channels, f can be expressed as a weighted average of the four-sided smooth channel friction factor f_{ss} , and the four-sided ribbed channel friction factor f_{rr} . On the basis of the previous assumption, the relationship between three friction factors, f , f_{ss} , and f_{rr} , is given by

$$f = (f_{rr} + f_{ss})/2 \quad (1)$$

The friction roughness function $R(e^+)$, and heat transfer roughness function $G(e^+)$, can be experimentally determined and correlated by f , and the ribbed wall Stanton number St_r , for fully developed turbulent flow in a square channel with nonrectangular ribbed walls.

According to Han,² the laws of the wall can also be applied to fully developed turbulent flow in rectangular channels with repeated-rib rougheners and with different channel aspect ratios. Thus, the friction and heat transfer similarity laws in

Received May 17, 1996; presented as Paper 96-1840 at the AIAA 31st Thermophysics Conference, New Orleans, LA, June 17-20, 1996; revision received July 11, 1997; accepted for publication July 11, 1997. Copyright © 1997 by the American Institute of Aeronautics and Astronautics, Inc. All rights reserved.

*Professor, Department of Mechanical Engineering.